Wind and Structures, Vol. 9, No. 5 (2006) 397-412
DOI: http://dx.doi.org/10.12989/was.2006.9.5.397

Response prediction of a 50 m guyed mast under typhoon conditions

S. S. Law†

Civil and Structural Engineering Department, Hong Kong Polytechnic University, Hunghom, Kowloon, Hong Kong, People's Republic of China

J. Q. Bu‡

Shijiazhuang Railway Institute, Shijiazhuang, Hebei, People's Republic of China

X. Q. Zhu‡† and S. L. Chan‡‡

Civil and Structural Engineering Department, Hong Kong Polytechnic University, Hunghom, Kowloon, Hong Kong, People's Republic of China

(Received September 21, 2005, Accepted August 18, 2006)

Abstract. This paper presents the wind excited acceleration responses of a 50 m guyed mast under the action of Typhoon Dujuan. The response of the structure is reconstructed from using a full finite element model and an equivalent beam-column model. The wind load is modelled based on the measured wind speed and recommendations for high-rise structures. The nonlinear time response analysis is conducted using the Newton Raphson iteration procedure. Comparative studies on the measured and computed frequencies and acceleration responses show that the torsional vibration of the structure is significant particularly in the higher vibration modes after the first few bending modes. The equivalent model, in general, gives less accurate amplitude predictions than the full model because of the omission of torsional stiffness of the mast in the vibration analysis, but the root-mean-square value is close to the measured value in general with an error of less than 10%.

Keywords: wind load; guyed mast; nonlinear; mode shape; acceleration; finite element model; typhoon; eigenvalue; equivalent model.

1. Introduction

This paper is a companion paper to Law, *et al.* (2006) which describes the wind characteristics of Typhoon Dujuan as measured in 2003 in Hong Kong. This paper presents the wind excited

† Associate Professor, Corresponding Author, E-mail: cesslaw@polyu.edu.hk
‡ Associate Professor
‡† Research Fellow
‡‡ Professor

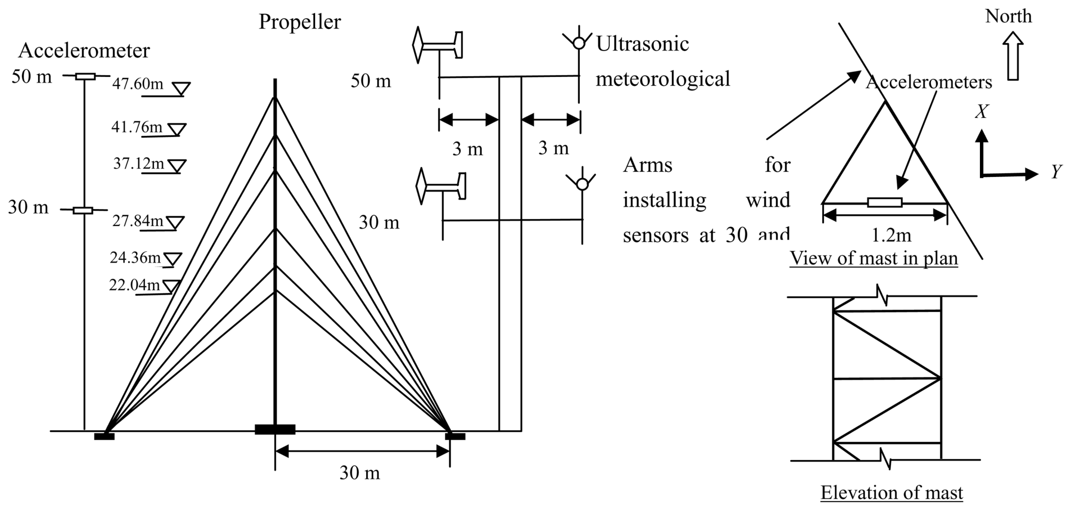

Fig. 1 Schematic view of the instrumented guyed mast

acceleration responses of a 50 m guyed mast under the typhoon action. A wind load model on the structure is developed based on the measured wind information and specifications from existing recommendations for high-rise structures. The dynamic responses of the structure under the action of the simulated wind load are reconstructed and compared with the measured responses. Structural model constructed from equivalent beam-column elements and a full finite element model of the structure are used. The non-linearity due to the sag of the cable, the second order axial force effect and the large displacement effect of the cables are included in the time response analysis and Newton Raphson method is used. This study aims to provide a reference on the design and fatigue life assessment of a guyed mast under typhoon conditions.

2. The guyed mast and instrumentation

The 50 m high mast has been described in detail in Law, *et al.* (2006), and a brief description is given here for clearity. It has an equilateral triangular cross-section 1.2 m long each side. The three vertical legs are of hollow steel tubes. The diagonals and horizontal members are also of steel tubes. Two arms 3 m long each, extend from the mast structure at 30 m and 50 m above ground level supporting the anemometers at the ends as shown in Fig. 1. The accelerometers are housed inside an instrument box on one of the sides of the triangle at these two levels to monitor the responses in two orthogonal directions i.e., the X- and Y- directions as shown. The Z- axis passes through the centroid of the cross-section of the guyed mast, and the origin of coordinates is set at the ground level.

3. Wind excited structural responses

The measured accelerations in the two perpendicular directions at 30 m and 50 m levels are plotted in Fig. 2(a). Acceleration from 50 m level has peak values larger than 1 m/s^2 in both the X- and Y-directions. At the beginning, the X-direction vibration is noted, in general, to be larger than that in the Y-direction since the wind direction is mainly from a bearing of 300^0 and is close to X-

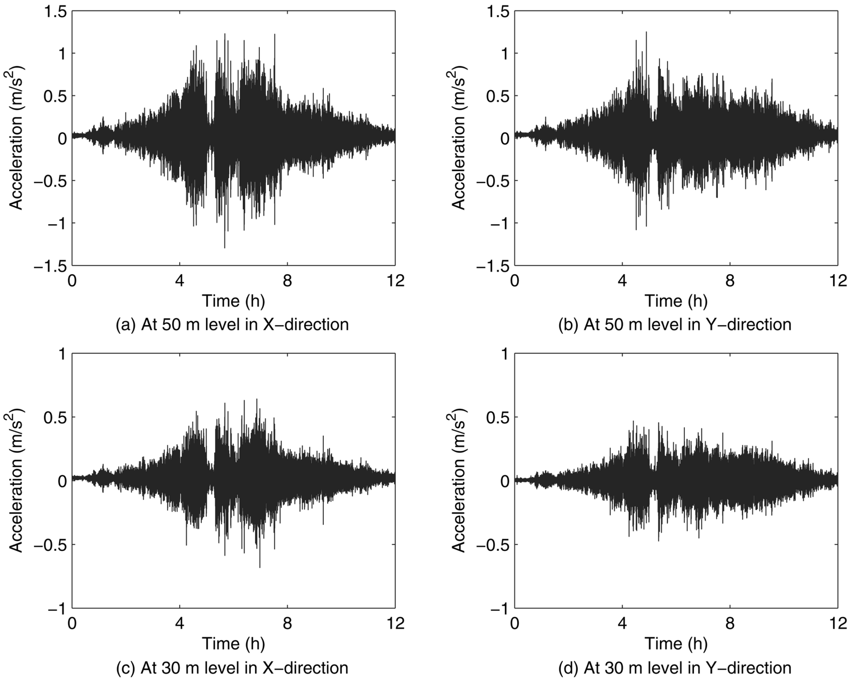

Fig. 2(a) Measured accelerations for 12 hours (from 14:00 2 Sept. to 02:00 3 Sept.)

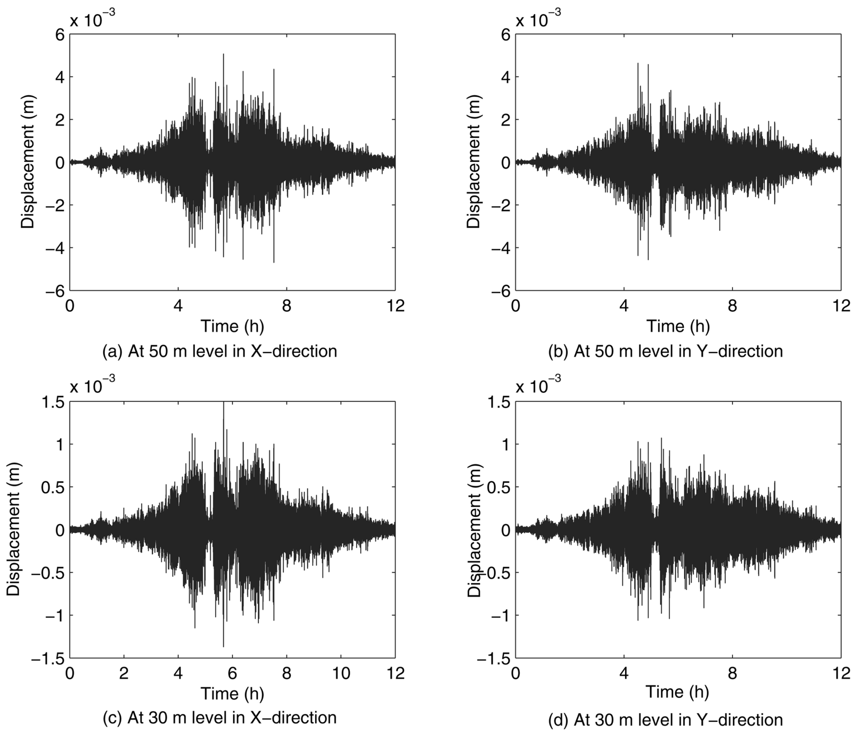

Fig. 2(b) Integrated displacements for 12 hours (from 14:00 2 Sept. to 02:00 3 Sept.)

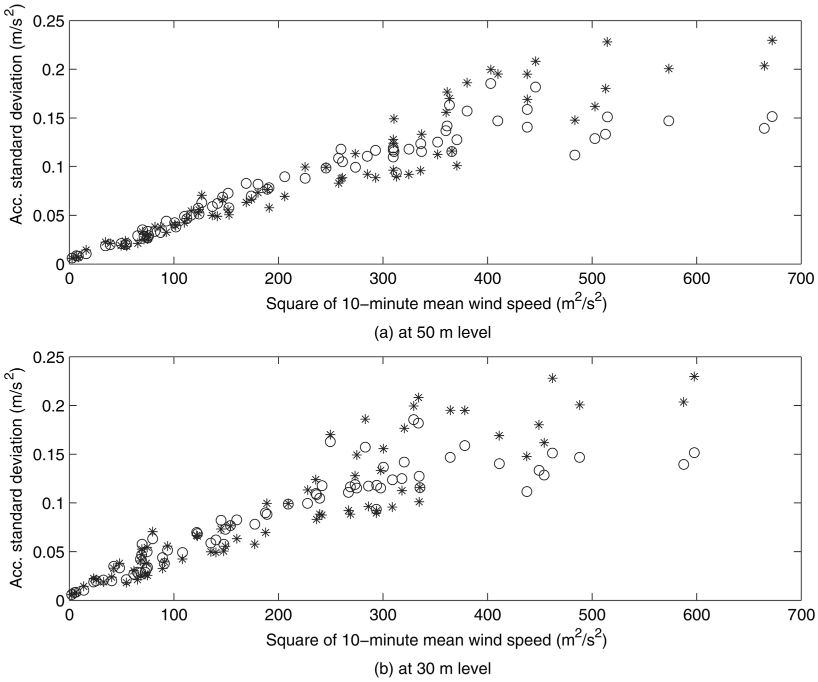

Fig. 3(a) Standard deviation of acceleration versus the square of 10-minute mean wind speed (o - in X-direction, * - in Y-direction)

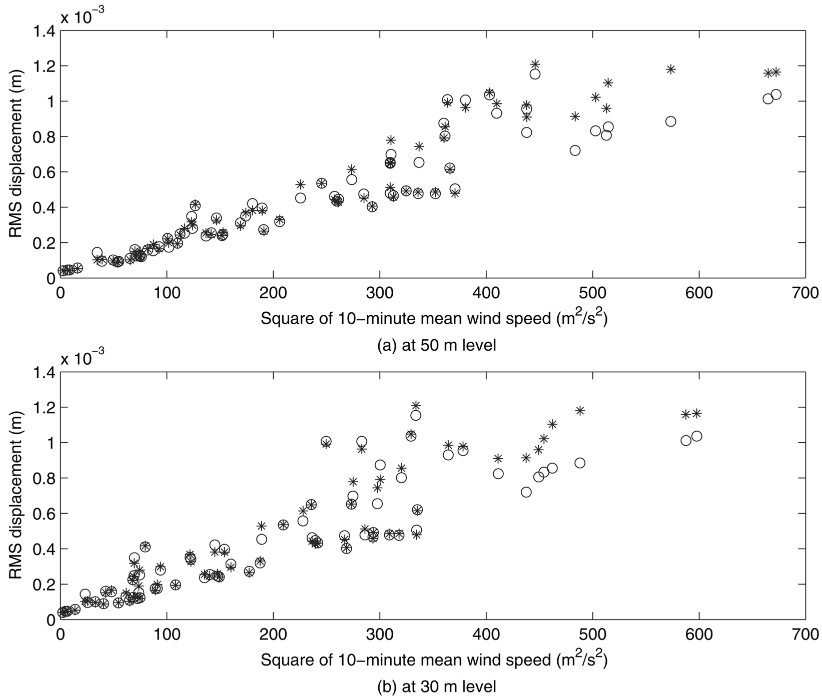

Fig. 3(b) RMS displacement versus the square of 10-minute mean wind speed (o - in X-direction, * - in Y-direction)

direction. But after 22:00 2nd September, the wind direction is mainly from a bearing of 160°, and the Y-direction vibration is larger than that in X-direction.

The displacement time histories evaluated from the double integration (Petrovski and Naumovski 1979) of acceleration time histories are plotted in Fig. 2(b). The displacement from 50 m level is noted to have peak values larger than 0.005 m in both the X- and Y- directions.

This study also examines the variation of acceleration and displacement responses of the guyed mast with 10-minute mean wind speed at 30 m and 50 m level. Fig. 3(a) shows the standard deviations of the measured acceleration responses of the guyed mast against the square of 10-minute mean wind speed. The variation in the acceleration increases with the energy of the wind and is nearly in linear proportion to the square of the mean wind speed. Fig. 3(b) shows the root mean square (RMS) value of the integrated displacement responses of the guyed mast against the square of 10-minute mean wind speed. The linear dependency of the two parameters is clearly observed indicating a proportional relationship between the amplitude and the wind energy input into the structure.

The auto-power spectrum of the acceleration responses and the damping ratio of the vibration modes are further studied using a selected length of measured data from both the typhoon and weak wind conditions. One hour measured data from under Typhoon Dujuan (22:00-23:00 2nd September), and one hour measured data from the weak wind record (16:00-17:00 12th September) are studied.

The auto-spectra of the measured acceleration responses are plotted in Figs. 4(a) and (b). The size of Fourier transforms is 1024 with a frequency increment of 0.0488 Hz between two adjacent data points. The spectra show clearly the closely spaced vibration modes of the structure. The

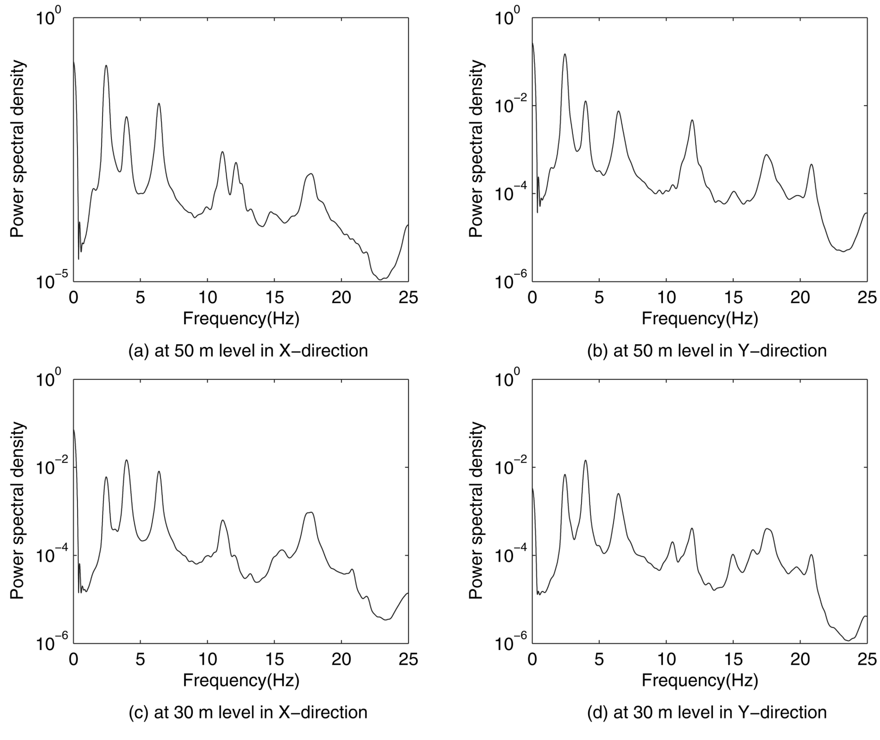

Fig. 4(a) Power spectral density of measured accelerations under Typhoon Dujuan

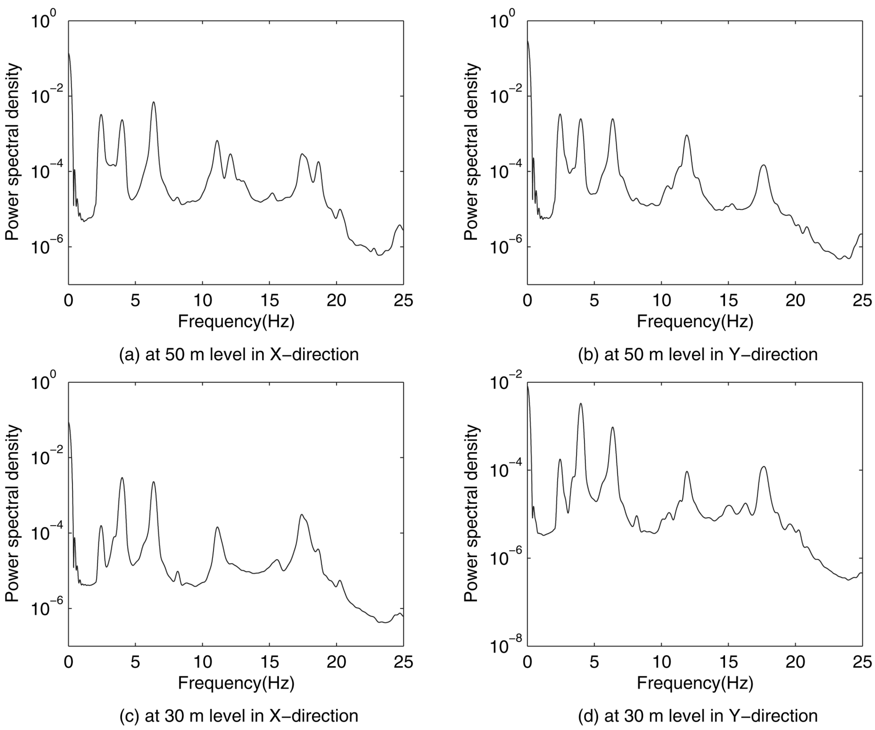

Fig. 4(b) Power spectral density of measured accelerations under weak wind conditions

Table 1 Comparison of the measured and calculated modal frequency (Hz)

Mode number		1	2	3	4	5	6	7	8	9	10	11
Measured under typhoon	X-50	2.43	4.19	6.38	10.85	11.91	15.20	17.14	-	-	-	20.21
	Y-50	2.40	3.95	6.34	10.72	11.52	14.99	17.00	-	-	-	20.43
	X-30	2.42	3.98	6.39	10.86	11.60	15.40	17.78	-	-	-	20.13
	Y-30	2.40	3.96	6.35	10.79	11.57	15.12	17.39	-	-	-	20.08
Measured under weak wind	X-50	2.41	3.95	6.39	11.23	11.77	15.52	17.59	-	-	-	20.03
	Y-50	2.40	3.93	6.28	-	11.73	-	17.00	-	-	-	20.05
	X-30	2.42	3.98	6.37	11.07	12.41	15.72	17.77	-	-	-	20.21
	Y-30	2.42	3.92	6.33	10.72	12.15	15.48	17.30	-	-	-	19.87
From full model		2.51	4.19	6.46	9.69	10.88	15.42	15.73	16.59	16.59	16.59	20.23
From equivalent beam-column model		2.51	4.11	6.51/ 7.11	10.39	10.69	16.27	16.53		-	-	20.29

Note: - denotes case not excited or not calculated.
X-50 denotes frequency from signal along X-direction at 50 m level.
Modes 8, 9 and 10 are axial modes.

frequencies identified from each of the spectra are shown in Table 1 after correlating with the analytical modal frequencies and the associated mode shapes. There are small differences between

Table 2 Identified modal damping ratios (%)

Number of mode		1	2	3	4	5	6	7	11
Under typhoon	X-50	1.14	0.54	0.43	0.28	0.26	0.19	0.14	0.19
	Y-50	1.23	0.81	0.26	0.18	0.15	0.12	0.15	0.10
	X-30	1.65	1.07	0.35	0.33	0.23	0.11	0.14	0.11
	Y-30	1.74	0.69	0.67	0.37	0.36	0.31	0.30	0.16
Under weak wind	X-50	1.22	0.45	0.45	0.39	0.33	0.22	0.09	0.12
	Y-50	1.39	0.78	0.53	-	0.21	-	0.13	0.12
	X-30	1.81	0.41	0.37	0.26	0.23	0.23	0.10	0.16
	Y-30	1.18	0.63	0.37	0.29	0.23	0.21	0.17	0.13

Note: - denotes case not excited.
X-50 denotes frequency from signal along X-direction at 50 m level.

the frequencies obtained from each spectrum, and it is difficult to determine a common value of the modal frequency because of the small number of measurements. Therefore the frequencies correspond to the peak values of each spectrum are shown as modal frequencies in Table 1.

The same modes are excited under the typhoon and weak wind conditions, but the frequencies obtained from each of the four accelerometers have small differences. The frequency obtained from the X-direction acceleration is, in general, larger than that from the Y-direction data. The axial vibration modes 8 to 10 cannot be found from the measurement. The frequencies obtained from the typhoon and weak wind conditions are similar, and this would indicate a weak nonlinearity in the guyed mast system even under the typhoon conditions.

The critical damping ratio for each mode is obtained by the half power point method, and is listed in Table 2 for the first eleven modes excluding the axial modes from one hour measured data for the two types of wind conditions (16:00-17:00, 2nd Sept. and 12th Sept.). The modal damping ratio decreases with the mode order. The largest value is 1.81% for the first mode in X-direction under weak wind conditions, and the values identified from typhoon conditions are in general smaller than those from weak wind conditions. This may be because the damping ratio decreases with vibration amplitude.

Since the structure is subjected to large wind force from the typhoon, a study on the variation of the damping ratio of the structure at the fundamental frequency with the mean wind speed is made. Fig. 5 shows the damping ratio plotted against the mean wind speed. The modal damping ratio scatters between 0.5% and 2.0% without a clear relationship with the mean wind speed. The average modal damping ratio is obtained as 1.44% and 1.35% for the X- and Y- directions at 30 m level respectively and 1.44% and 1.25% for the X- and Y- directions at 50 m level respectively. It is noted that the damping characteristics of the guyed mast depend on the non-linearity of the guys and the mast, materials, cross-section, type of joint, erection process and vibration amplitude, etc., and are very complicated (Wang 2001).

4. Structural models

Many previous researchers used an equivalent model for the guy mast. The mast was characterized as a beam on elastic supports and the guy support was treated as an equivalent spring-

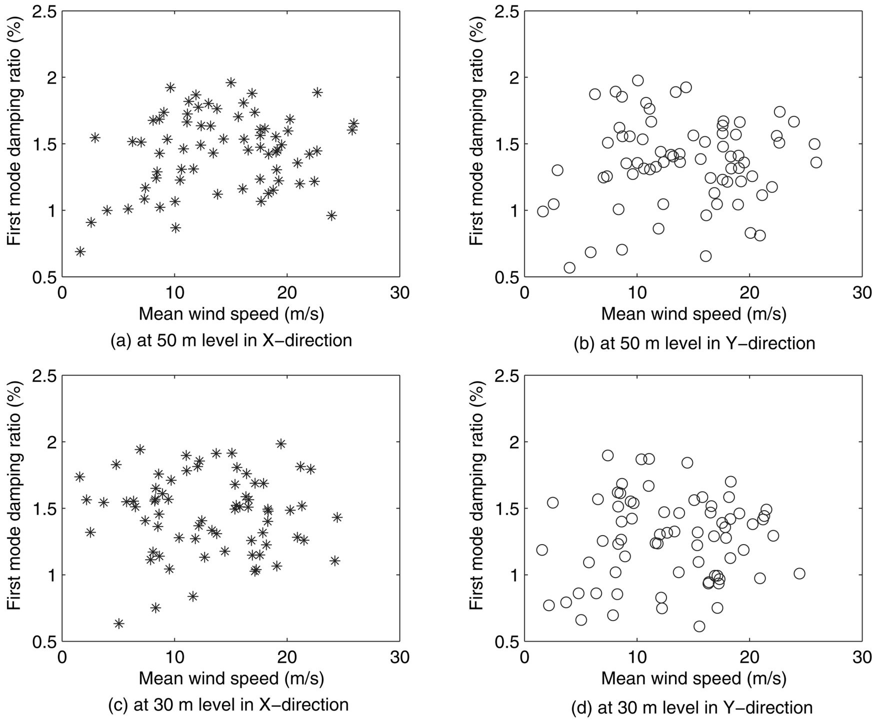

Fig. 5 Variation of first modal damping ratio with 10-minute mean wind speed (* - in X-direction, o - in Y-direction)

mass-spring system (Gerstoft and Davenport 1986). Cohen and Perrin (1957) treated the guyed tower as a continuous beam-column on elastic supports, with the spring stiffness from the guys attached to the mast. However, their two-dimensional idealization of the tower considered only flexural stiffness. Kahla (1995) developed a three-dimensional beam-column element which incorporates the axial, flexural, shear and torsional stiffnesses of cross-section of a mast built from multiple triangles. Both the equivalent model and the full finite element model outlined below are used in the eigenvalue and dynamic response analysis.

4.1. Full model

This model consists of 129 beam-column elements representing the chord members and 258 truss elements representing the diagonals and horizontal members. The cables are represented by 108 two-node catenary cable elements (Pan and Fan 1998). This model has 1044 degrees-of-freedom and is used as a reference for comparison with the simplified beam-column model shown below. The legs of the mast are fixed at the bottom while the cables are pinned at the anchor blocks.

4.2. Equivalent beam-column model

A segment of the mast is modeled by an equivalent beam-column element. Three types of equivalent elements are used to model the whole length of the guyed mast as shown in Table 3. The beam-column representing a length of mast of 2.32 m, 3.48 m or 3.6 m long with one end fixed and

Table 3 Equivalent properties of the equivalent beam-columns

Equivalent stiffness	Member location		
	0 m ~ 5.8 m	5.8 m ~ 46.4 m	46.4 m ~ 50.0 m
Axial area-A (m^2)	3.27×10^{-3}	2.67×10^{-3}	2.67×10^{-3}
Second moment of area-I_{xx} (m^4)	3.73×10^{-3}	2.06×10^{-3}	2.00×10^{-3}
Second moment of area-I_{yy} (m^4)	3.73×10^{-3}	2.06×10^{-3}	2.00×10^{-3}
Torsional moment of area-J (m^4)	2.67×10^{-4}	2.61×10^{-4}	2.57×10^{-4}
Shear area-A_{xx} (m^2)	1.17×10^{-3}	1.17×10^{-3}	1.15×10^{-3}
Shear area-A_{yy} (m^2)	1.17×10^{-3}	1.17×10^{-3}	1.15×10^{-3}

the other end free. A moment is applied at the free end along the global X-direction and the resulting deformation is calculated, from which the flexural stiffness is estimated. This is repeated for a shear force, an axial force and a torsional moment to get the equivalent shear, axial and the torsional stiffnesses. The properties along the Y-direction are similarly obtained. The properties calculated according to Kahla (1995) for a mast with equilateral triangular cross-section are listed in Table 3. There are two beam-column segments below 5.8 m and eighteen segments above 5.8 m, and the above process is repeated for each segment to get the beam-column element properties. This simplified model consists of 20 beam-column elements representing the mast, 90 truss elements representing the cables, and 18 truss elements with rigid arm (Wu and Ren 2000) that links up the cable/mast connection points to the centre of the equivalent beam-column elements. There is a total of 444 degrees-of-freedom in this model.

4.3. Geometric nonlinearity

The guyed mast is a flexible structure exhibiting geometric non-linearities under wind load. The nonlinearity mainly comes from the sag effect of cable, the axial force effect and large displacement effect.

The sag effect of cable is taken care of by adopting the equivalent tangential elasticity modulus E_{eq} proposed by Ernst (1965). Geometric stiffness matrix is considered in the final stiffness matrix by including the axial force effect. The large displacement effect in the computation of dynamic response under load is considered by adopting the Newton Raphson method in the updating of the system stiffness matrix and the displacement vector iteratively.

5. Modal analysis

The self weight and initial pre-stressing forces are applied on the structure, and equilibrium is achieved resulting in a deflected shape which is adopted as the initial shape of the structure. The natural frequencies and corresponding mode shapes of the guyed mast are then computed through eigenvalue analysis. The first 100 natural frequencies and mode shapes are obtained. Since the cable is much more flexible than the mast in both finite element models, those modes involve no interaction between the cables and the mast are removed leaving behind the “purely mast” modes and modes with strong coupling between the cables and the mast, and the natural frequencies from both structural models are listed in Table 1. Since the flexural rigidities along the X- and Y-directions of the structure are the same, the vibration modes with major bending motion about each of the two axes are very close, and most of them are usually coupled with torsion in the cross-section in the case of the full model. The flexible horizontal arms at the equipment levels are replaced with an equivalent lumped mass at the root to suppress the many low frequency vibration modes dominated by their vibration. The instrument boxes and the anemometers are modeled as lumped masses, and the stiffness of the cat ladder is ignored in the study.

The first twelve mode shapes calculated from the full model but excluding the axial modes 8 to 10 are plotted in Fig. 6. The first, second and the fourth modes are dominated with bending motion, and the rest except the last one, have strong coupling between the bending and torsion motion. The last mode has coupling between the bending and axial motion.

The frequencies obtained from the equivalent model are in general larger than those form the full model. The two modal frequencies shown for the third mode from the equivalent model have very similar mode shapes. The calculated frequencies from both models agree well with the measured values, especially in the first three modes. Both models are used in the following time response analysis under the wind load excitation.

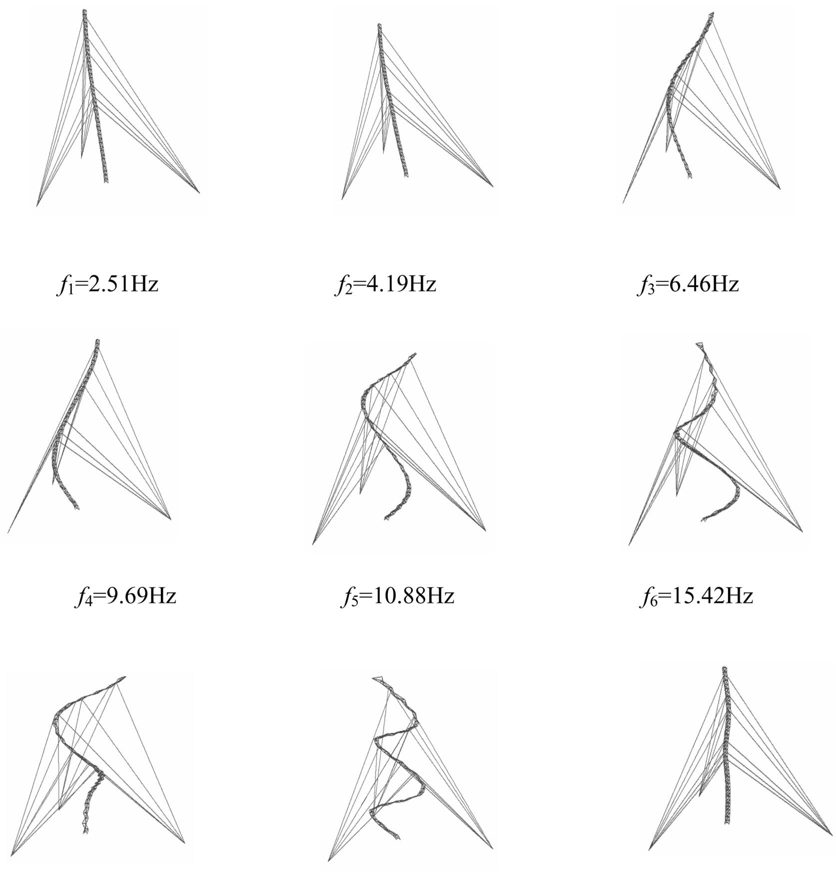

f_1=2.51Hz f_2=4.19Hz f_3=6.46Hz

f_4=9.69Hz f_5=10.88Hz f_6=15.42Hz

f_7=15.73Hz f_{11}=20.23Hz f_{12}=21.45Hz

Fig. 6 Analytical vibration mode shapes of the guyed mast

6. Wind load on the mast

The wind pressure on the structure is computed with reference to the local wind conditions (Liu 1991). The vertical distribution of wind speed is assumed to follow the power law (Specification 1991). The reference height is taken to be 30 metres. Fifteen lengths of wind data covering periods of typical strong wind conditions each for 10 minutes at 30 m and 50 m level are used to find the power law exponent, and the average value is 0.11. The exponent for the weak wind conditions is similarly found to be 0.08. This vertical distribution of mean wind speed will be used to approximate the mean wind speed at different heights along the structure for simulating the wind load input on the structure later.

The wind pressure w is related to the wind speed by

$$w = \frac{\gamma}{2g}v^2 \tag{1}$$

where v is wind speed, g is the acceleration of gravity and γ is the unit weight of air. Because Hong Kong is on the south-east coast of China, the coefficient of wind pressure $\gamma/2g$ can be selected as 1/1700 according to reference (Zhang 1985).

Since the mast structure has a non-varying profile along its height, the equivalent exposed area per unit height, A_0, could be taken as constant and is calculated as Kahla (1995),

$$A_0 = \left(3\frac{\sqrt{3}}{4}\tan\theta\right)D_s + \left[\cos^2\theta + \frac{2}{\cos\theta}\left(1 - \frac{1}{4}\sin^2\theta\right)^{\frac{3}{2}}\right]D_d + 3D_c \tag{2}$$

where D_s, D_d and D_c are the diameters of the struts, diagonals and chords, respectively. θ is the angle between the diagonals and chords of the mast. If the full model is used to analyze the dynamic responses of the structure, the exposed area is reduced by one-third.

The wind load acting on the ith segment of the mast, F_i, can be finally computed as

$$F_i = wA_0L_i\mu_s = \frac{1}{1700}A_0L_i\mu_s v^2 \tag{3}$$

where coefficient μ_s is a function of the type of cross-section as well as the projected area of the structure orthogonal to the wind direction, and it can be obtained from the specification for high-rise structures (Specification 1991). L_i is the vertical length of the ith segment. $v = \bar{v}_z + v_{zf}$, where $\bar{v}_z$ is the mean wind speed at the ith segment which can be calculated according to the power law. v_{zf} is the fluctuating wind speed at height z. It is taken as v_{50f} for sections above 30 m, and v_{30f} for sections below 30 m. F_i is shared equally between the two ends of the segment. Wind load acting on the cable can also be calculated using Eq. (3) by replacing A_0 with the diameter of the cable.

The wind loads acting at different nodal points of the structure are then grouped into a time-varying load matrix for the subsequent response analysis.

7. Comparison between the measured and calculated responses

He, *et al.* (2003) have recently proposed a discrete analysis method for calculating the stationary or non-stationary random vibration responses of a guyed mast. It discretizes the

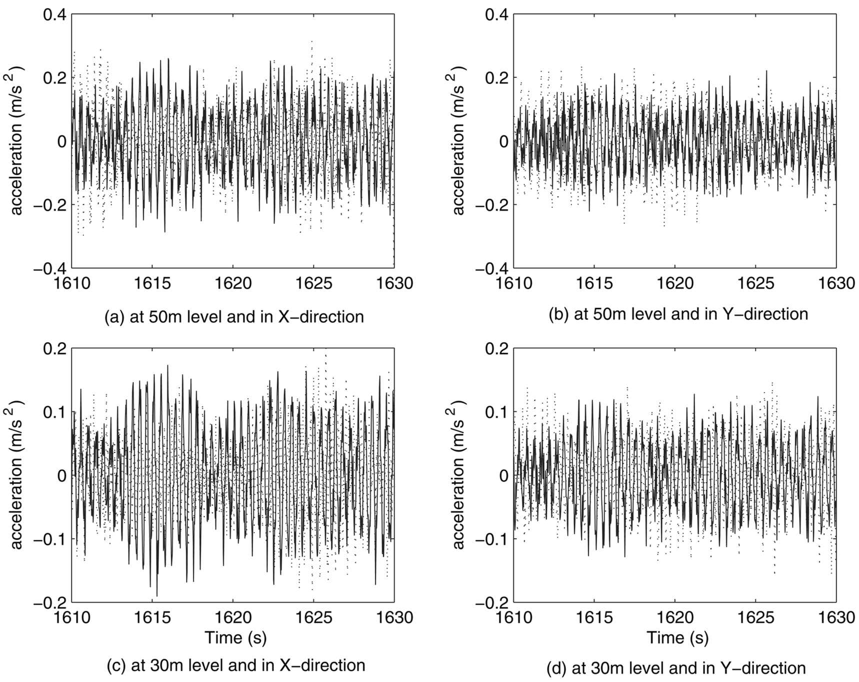

Fig. 7(a) Comparison between the measured and calculated accelerations (18:00 2nd Sept.) due to northwesterly wind (- - - - measured, —— calculated from full model)

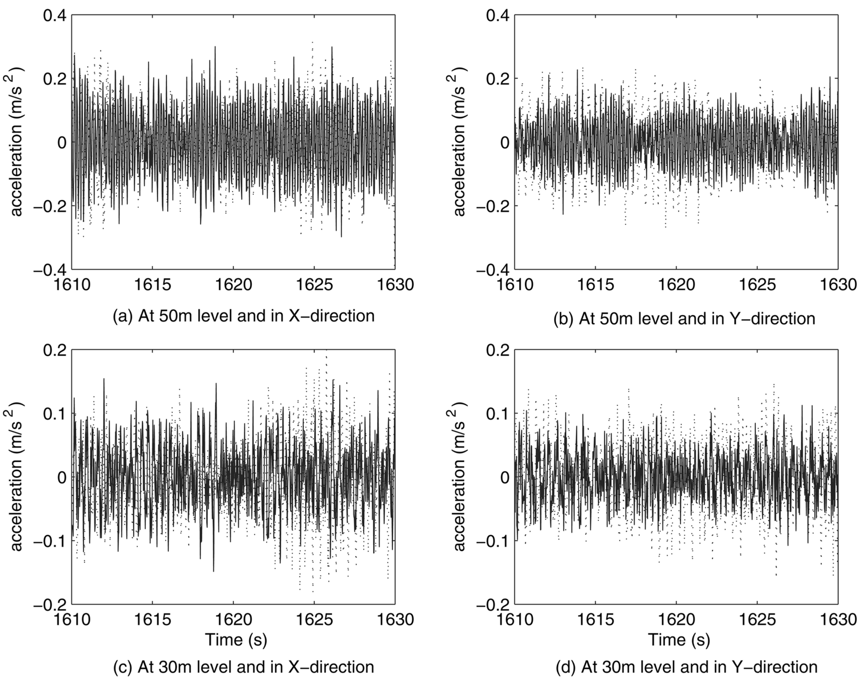

Fig. 7(b) Comparison between the measured and calculated accelerations (18:00 2nd Sept.) due to northwesterly wind (- - - - measured, —— calculated from equivalent model)

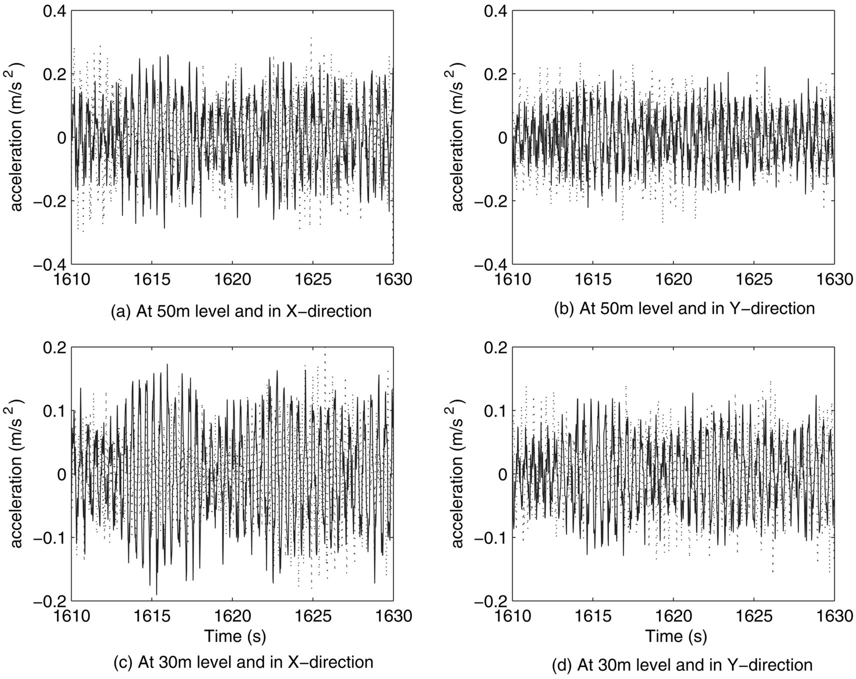

Fig. 7(c) Comparison between the measured and calculated accelerations (23:00 2nd Sept.) due to southeasterly wind (- - - - measured, —— calculated from full model)

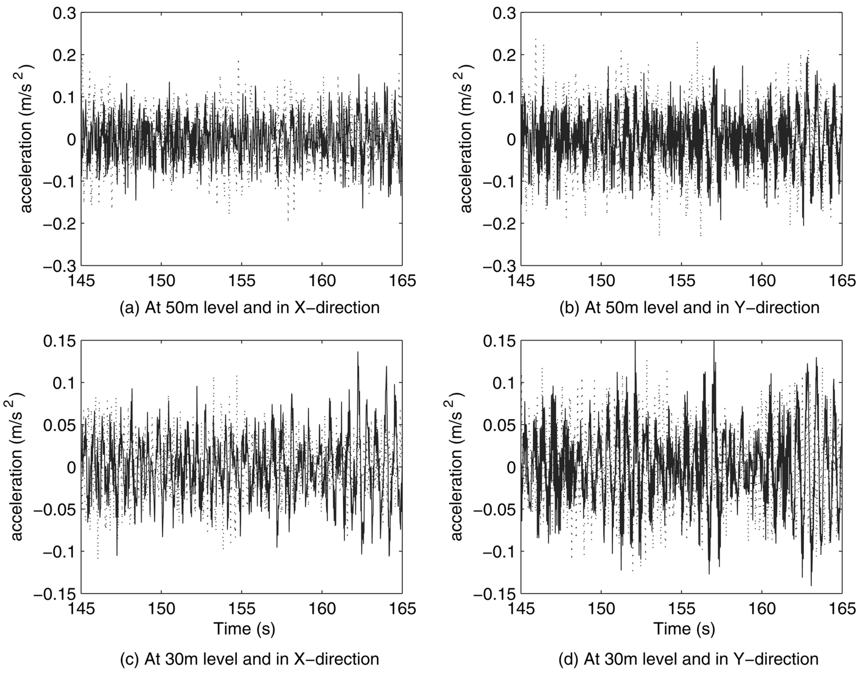

Fig. 7(d) Comparison between the measured and calculated accelerations (23:00 2nd Sept.) due to southeasterly wind (- - - - measured, —— calculated from equivalent model) vibration equation in the time domain, and uses the mean process and correlation characteristics of the excitations to calculate the mean and mean square random vibration responses. But it is only good for white noise excitation. The Newton Raphson method is therefore used in the present time response analysis.

A period of 20 seconds starting at 1610 second in 18:00 hour on 2^{nd} September is selected for the study. This corresponds to a northwesterly wind at an average speed of 19.82 m/s and direction of 290.15°. The wind load on the guyed mast is computed from the measured wind direction and speed. The accelerations are calculated using a time increment of 0.02 second, and the recorded wind data is interpolated to have the same time increment. Results from both the full model and the simplified model are plotted in Figs. 7(a) and (b). Another 20 seconds period starting at 145 second in 23:00 hour on 2^{nd} September 2003 which corresponds to a southeasterly wind at an average speed of 18.05 m/s and direction of 168.84° is also studied. The results are plotted in Figs. 7(c) and (d).

The calculated time responses do not match perfectly with the measured responses but with roughly the same time cycle since the response is dominated by the first few modes which are closely predicted by the analytical finite element models. The first one or two seconds of the computed time history should be less accurate than the rest because of the presence of non-zero initial conditions in the computation. But this effect is a transient and it will diminish to zero in a few seconds.

Results in Fig. 7 show that the calculated accelerations from both models match the measured accelerations approximately either under the southeasterly or northwesterly wind. The calculated and measured accelerations exhibit similar behaviour, and they have the same peaks and valleys at approximately the same time, and their maximum values are close to each other.

The root-mean-square (RMS) value of the integrated displacements from the measured and calculated accelerations shown in Fig. 7 are computed and listed in Table 4. Those from the computed accelerations are very close to those from the measured accelerations, and the equivalent model gives, in general, smaller response than the full model. This may be because the equivalent model neglects the torsional stiffness of the mast resulting in a stiffer structure and consequently smaller vibration responses. This confirms the observation in the calculated modal frequencies in Table 1 where those obtained from the equivalent model are in general larger than those from the full model.

Table 4 Root-mean-square values (mm) of the integrated displacements from the measured and calculated accelerations

Time duration	Type	Position and direction			
		X-50	Y-50	X-30	Y-30
1610s-1630s in 18:00 hour 2^{nd} Sept.	From measurement	2.04	1.81	0.84	0.79
	From full model	2.19 | 7.5	1.75 | -3.3	0.94 | 12.2	0.85 | 6.9
	From equivalent model	1.93 | -5.4	1.66 | -8.2	0.79 | -4.9	0.68 | -13.8
145s-165s in 23:00 hour 2^{nd} Sept.	From measurement	1.02	1.22	0.56	0.62
	From full model	1.07 | 4.8	1.28 | 4.6	0.60 | 7.5	0. 59 | -4.5
	From equivalent model	0.93 | -9.1	1.12 | -8.1	0.52 | -6.3	0.57 | -7.9

Note: •|• denotes the calculated value|error (%) relative to the measured value; X-50 means at 50 m in X-direction

8. Conclusions

This paper presents the wind excitation responses of a 50 m guyed mast under the effect of typhoon conditions. The responses are reconstructed based on a wind load model developed from measured wind speed and recommendations for high-rise structures. Newton Raphson method is used in the analysis with a full finite element model and an equivalent beam-column model of the structure. The nonlinearities of the system have been included in the analysis. The following conclusions can be drawn from this study.

The acceleration and the integrated displacement of the guyed mast are in linear proportion to the square of the 10-minute mean wind speed which may be used as a reference for design purposes.

The torsional vibration of the structure is significant particularly in the higher vibration modes after the first few bending modes. The full finite element model and the equivalent model could be used for the prediction of the dynamic response under wind load with a larger error with the latter model due to the omission of the torsional stiffness in the structure. The RMS values are however very close to the measured values in general with an error of less than 10%.

The calculated natural frequencies from two models compare well with the experimental values indicating that both models are satisfactory in predicting the flexural vibrations. The equivalent model has a much reduced number of degrees-of-freedom and its use would result in appreciable savings in computation time.

Acknowledgements

The work described in this paper was supported by a grant from the Hong Kong Research Grant Council Project No. PolyU 5043/02E. Acknowledgement is made to the Highways Department of the Hong Kong Special Administrative Region Government for its permission to make use of the measured data from the guyed mast for the present research and this publication.

References

Ben Kahla, N. (1995), "Equivalent beam-column analysis of guyed towers", *Comput. Struct.*, **55**(4), 631-645.
Cohen, E. and Perrin, H. (1957), "Design of multi-level guyed towers: Structural analysis", *J. Struct. Div.,* ASCE, **83**(5), 1356-1-1356-29.
Ernst, H. J. (1965), "Der E-modul von seilen unter berucksichtigung des durchhanges", *Der Bauingenieur*, **40**(2), (in German).
Gerstoft, P. and Davenport, A. G. (1986), "A simplified method for dynamic analysis of a guyed mast", *J. Wind Eng. Ind. Aerodyn.*, **23**, 487-499.
He, Y. L., Ma, X., and Wang Z. M. (2003), "Nonlinear discrete analysis method for random vibration of guyed masts under wind load", *J. Wind Eng. Ind. Aerodyn.*, **91**, 513-525.
Law, S. S., Bu, J. Q., Zhu, X. Q., and Chan, S.L. (companion paper) (2006), "Wind characteristics of typhoon dujuan as measured at a 50 m guyed mast", *Wind and Struct., An Int. J.*, **9**(5), 387-396.
Liu, H. (1991), *Wind Engineering-A Handbook for Structural Engineering*, Prentice Hall, Englewood Cliffs, New Jersey. 42-43.
Pan, Y. R. and Fan, L. C. (1998), "Application of catenary element to calculating the fabrication length of main cable of suspension bridges", *Structural Engineers*, **1998**(3), 20-24
Petrovski, J. and Naumovski, N. (1979), "Processing of strong motion accelerograms. Part 1: Analytical methods", Report 66. I211S, Stronjze.
Specification for High-Rise Structure Design (GBJB5-90) (1991), China Construction Industry Publishing House,

Beijing, PCR.
Wang, Z. M., Wang, Z. H., and Yan, M. Z. (2001), *Guyed Mast Structure*, Science Publishing House, Beijing, PCR.
Wu, H. Q. and Ren, X. (2000), *Finite Element Analysis for Structure*, China railway Publishing House, Beijing, PCR.
Zhang, X. T. (1985), *Calculation of Wind Pressure on Structure and Wind-Induced Vibration*, Tongji University Publishing House, Shanghai, PRC.

CC